Applied Physics B (2018) 124:92
https://doi.org/10.1007/s00340-018-6952-7

Applied Physics B
Lasers and Optics

Nanosecond-pulsed Q-switched Nd:YAG laser at 1064 nm with a gold nanotriangle saturable absorber

Xiaohan Chen[1] · Ping Li[1] · Yangyang Dun[1] · Teng Song[1] · Baomin Ma[1]

Received: 2 June 2017 / Accepted: 13 April 2018 / Published online: 4 May 2018

Abstract
Gold nanotriangles (GNTs) were successfully employed as a saturable absorber (SA) to achieve passively Q-switched lasers for the first time. The performance of the Q-switched Nd:YAG laser at 1064 nm has been systematically investigated. The corresponding shortest pulsewidth, the threshold pump power and the maximum Q-switched average output power were 275.5 ns, 1.37 W, and 171 mW, respectively. To our knowledge, this is the shortest pulsewidth and the lowest threshold in a passively Q-switched laser at approximately 1.1 μm based on a gold nanoparticle SA (GNPs-SA). Our experimental results proved that the GNTs-SA can be used as a promising saturable absorber for nanosecond-pulsed lasers.

1 Introduction

All solid-state Q-switched lasers are desirable for various applications, such as laser ranging environment sensing, communication, military, medical treatment, and industrial material processing, due to their high peak power and pulse energy [1–3]. Q-switching lasers can be obtained via two approaches, a passive method and an active method. Passively Q-switched solid-state lasers that use saturable absorbers have wide applications in fields of remote sensing, scientific research, medicine due to their advantages of potentially simplicity, and lower cost in fabrication and operation compared to the active method [4–6]. Obviously, developing new saturable absorber materials with low cost, broad absorption band, and low intrinsic loss is crucial to achieve high-quality laser performance. Several types of SAs have been successfully employed to realize pulsed lasers such as Cr^{4+}:YAG, semiconductor saturable absorption mirrors (SESAM), GaAs, and so on [7–9]. However, these SAs have disadvantages such as complexly fabrication and narrow absorption band. In recent years, graphene and graphene oxide have been successfully used in the wavelength region from the visible to the terahertz due to its zero band-gap structure [10]. Compared with zero band-gap graphene, 2D-layered transition metal dichalcogenides (TMDs), e.g., MoS_2, $MoSe_2$, and WS_2, whose band-gap changes from indirect to direct band-gap semiconductor as it is getting thinner [11–13]. Based on those 2D materials as SA, near-infrared passively Q-switched lasers have been experimentally demonstrated, which indicates the great potential of 2D materials for 1 μm pulsed lasers.

Recently, as another kind of 2D material, gold nanoparticles (GNPs) and their compounds have been of particular interest to researchers because of their large third-order nonlinearity and fast recovery time. According to Refs. [14, 15], the nonlinear saturable absorption effect of GNPs is a result of ground-state plasmon bleaching. Gold nanobipyramids (GNBPs) and gold nanorods (GNRs) have been experimentally proven to be usable as saturable absorbers for passively Q-switched lasers. In 2016, Zhang and Liu demonstrated an all-solid Q-switched laser using GNBPs with a pulsewidth of 396 ns and a Q-switched threshold of 7 W at 1.1 μm [16]. In 2013, Kang et al. achieved a 4.8 μs Q-switched and 12 ps mode-locked erbium-doped fiber laser using GNRs [17, 18]. In addition, in Ref. [19], GNRs with a longitudinal surface plasmon resonance (SPR) peak at 1063.8 nm were fabricated and experimentally exploited as the single and combined SA in a Q-switched Nd:YAG laser. In 2017, Feng et al. achieved a maximum output power of 54 mW at 1061 nm in an Nd:GAGG laser using GNRs as a saturable absorber [20]. Compared with the other aforementioned GNPs, gold nanotriangles (GNTs), a new kind of nanomaterial, have been attracting increasing attention because of their unique

✉ Baomin Ma
baominma@163.com

[1] School of Information Science and Engineering and Shandong Provincial Key Laboratory of Laser Technology and Application, Shandong University, Jinan 250100, People's Republic of China

optical properties and the new development of large-scale preparation. GNTs are promising anisotropic nanoparticles due to their triangle structure, their structure- and environment-dependent optical features, their anisotropic surface energetics, and the emergence of reliable synthetic methods for their producing with control of their edge length and thickness ratios. In addition, their sharp edges provide "hot-spots" that enhance surface-enhanced Raman spectroscopy (SERS)-sensing abilities [21–25]. Longitudinal SPR is the main features of plasmonic GNPs. For different sizes of GNTs, the longitudinal SPR band varies over different ranges [26]. By adjusting the aspect ratio in the reaction, the extinction spectra can be regulated and extended from the visible region to the near-infrared region. Furthermore, the recovery time of GNTs is typically on a fast timescale of a few picoseconds because of the electron–phonon and phonon–phonon interaction processes. These properties make GNTs promising SAs. However, there have been few demonstrations of the use of GNTs as SAs in passively Q-switched lasers.

In this letter, to the best of our knowledge, a GNTs-SA grown by the seed-mediated growth method was successfully fabricated, and the passive Q-switching operations of a diode-end-pumped Nd:YAG laser at 1.1 μm with GNTs-SA were realized for the first time. By accurately controlling the aspect ratios, the absorption peak of the GNTs was measured to be at 1092 nm. The minimum pulsewidth and the threshold pump power of the Q-switched lasers were 275.5 ns and 1.37 W, respectively. Compared with the previous results, this pulsewidth is much shorter, and the threshold pump power is much lower [16, 19].

2 The fabrication and characterization of the GNTs-SA

The GNT solution was provided by the JCNANO Corporation. GNTs were synthesized by the seed-mediated growth method. First, 0.1 ml of 24.33 mM $HAuCl_4{\cdot}4H_2O$ solution and 0.25 ml of 10 mM sodium citrate solution were added sequentially to ultra-pure water. Then, 0.3 ml of 100 mM $NaBH_4$ solution was added rapidly to the mixture solution, and the mixture was stirred vigorously at 25 °C for 2 min to obtain the orange–red seed solution. The seed solution was kept at 25 °C for 2 h and was then used for growing the GNTs. The growth solution was prepared by mixing 100 ml of 0.2 M cetyltrimethyl ammonium bromide (CTAB), 2 ml of 24.33 mM $HAuCl_4$ solution, and 200 ml of deionized water in a flask. After the solution was mixed, 30 ml of 0.5 mM KI solution and 4 ml of 0.1 M Vc solution were added. When the color of the growth solution changed from dark nankeen to colorless, 4 ml of the seed solution was added to the growth solution at 25–30 °C. The final solution was kept at room temperature for more than 4 h to completely obtain the GNTs; then, 0.1 M NaCl was added to the final solution. After 12 h, the supernatant was removed. Then, pure water was added to the flask, and the color of the solution immediately changed from transparent to green. This change in color indicated the formation of GNTs.

Figure 1a shows the transmission electron microscopy (TEM) image of the prepared GNTs; Fig. 1b shows the absorption spectra of the GNT aqueous solution. The GNT solution has two absorption peaks at 754 and 1092 nm. The 754 nm peak and the 1092 nm peak were caused by the transverse SPR and the longitudinal SPR, respectively. The side of each GNT was 140 ± 20 nm, and the thickness was 8 ± 2 nm. The solution was prepared on a K9 glass sheet with a length and width of 1 and 10 mm, respectively. After the samples were kept in a vacuum drying oven, the SA was successfully fabricated. The dependence of the transmission ratio of the GNTs-SA on the pump power density was measured using the Z-scan technique. As described in Fig. 1c, the open-aperture Z-scan curve shows the modulation depth, nonbleachable loss, and saturable intensity, which were calculated to be ~ 16.1, 49%, and 0.24 MW/cm^2, respectively. This result indicates that the GNTs-SA can be used to induce Q-switching.

3 Experiment setup

A concave-plane configuration resonator cavity (shown in Fig. 2) was designed with a total length of 27 mm. A narrow-linewidth 808 nm fiber-coupled laser diode with a core diameter of 200 μm and a numerical aperture of 0.22 was used as the pumping source. After a 1:1 coupling lens system, the pump laser was coupled to the Nd:YAG crystal. The rear mirror M1 was a concave mirror with a curvature radius of 1000 mm. Both sides of the concave mirror were coated with an antireflection coating for the 808 nm wavelength, and the concave surface was coated with a high-reflection coating for the 1064 nm wavelength. The output coupler M2 was a flat mirror with a partial transmission of 10.8% at 1064 nm. An Nd:YAG crystal with a Nd^{3+}-doping concentration of 1.0 at.% and dimensions of $\Phi 4 \times 8$ mm^3 was used as the gain medium. Both ends of the laser crystal were antireflection-coated for the 1064 and 808 nm wavelengths. The laser crystal was wrapped with indium and placed in a copper block that was surrounded by cooling water, which remained at 19 °C. The SA with an initial transmission of 36.8% at 1064 nm was placed as close to the output coupler as possible. The output power was measured by a power meter (Molectron PM10) connected to a Molectron EPM2000. The pulsewidth and repetition rate of the laser

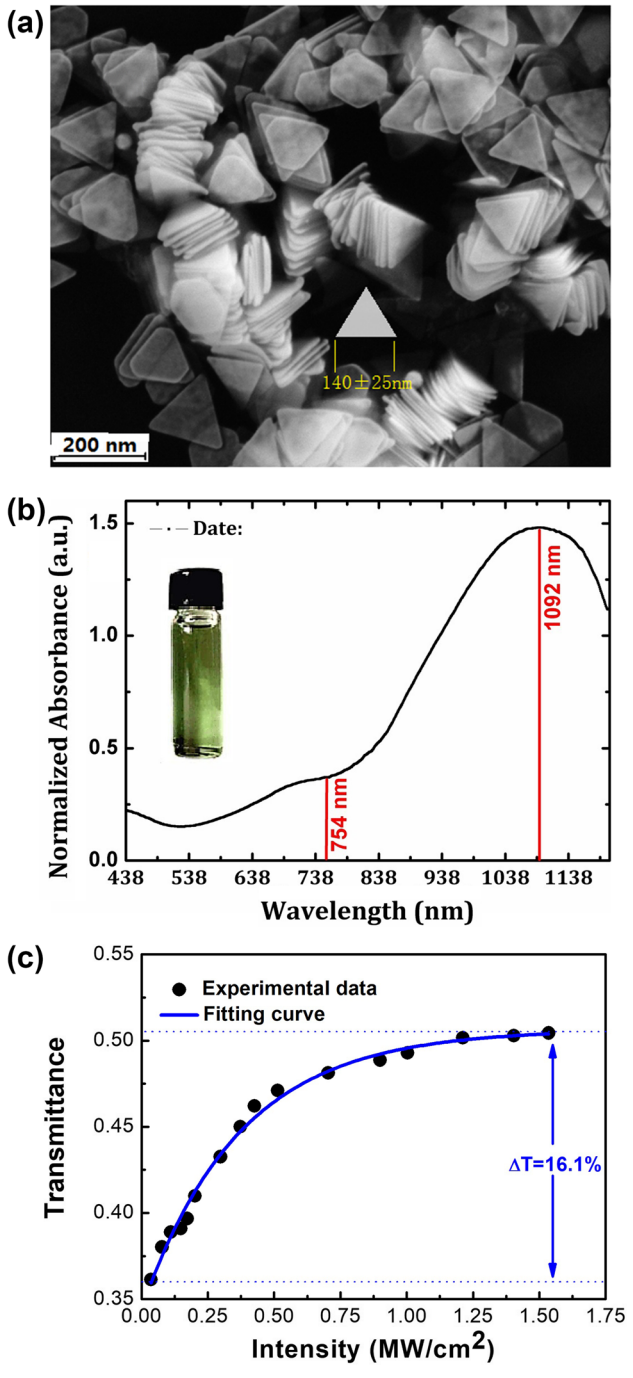

Fig. 1 **a** TEM image of the as-prepared GNTs; **b** the absorption spectra of the GNT aqueous solution and a picture of the GNT solution. **c** Saturable absorption characteristic of GNTs-SA at 1.1 μm

pulses were recorded by an Infiniium DSO90804A digital storage oscilloscope (8 GHz bandwidth, 40 G samples/s) and a fast PIN photodiode (1 GHz bandwidth).

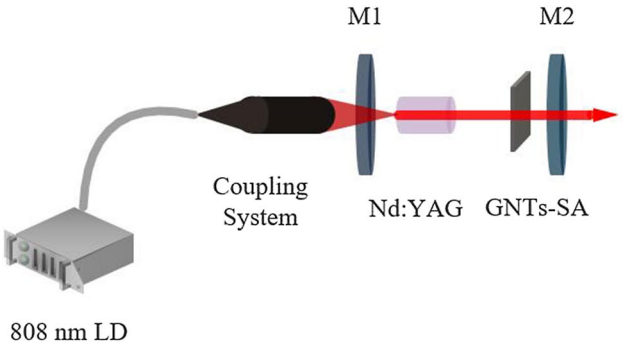

Fig. 2 Diagram of the Q-switched laser experimental setup

4 Results and discussion

First, the performance of the 1.06 μm continuous wave (CW) laser was investigated. The threshold of the laser was 322 mW. The 1064 nm laser output power increased linearly as the absorbed pump power was augmented. Without inserting the SA, a 4.31 W output power CW laser was obtained at a pump power of 12.56 W. When the pump power was increased continuously, the output power also increased linearly. The relationship between the incident pump power and the output power is shown in Fig. 3. The slope efficiency of the 10.8% output coupler was 35.2%. The central wavelength was 1064.3 nm as measured by a commercial spectrum analyzer (AQ 6315A) produced by Yokogawa, as shown in Fig. 4.

To study the performance of the passively Q-switched laser, the GNTs-SA was inserted into the cavity. For passively Q-switched operation, the threshold pump power increased to 1.37 W, and the average output power was

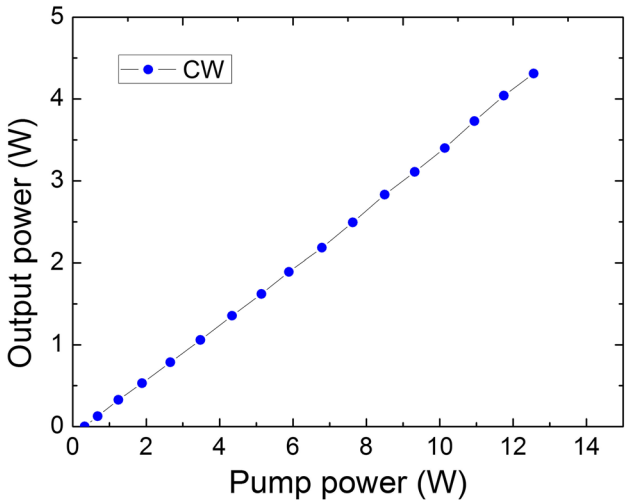

Fig. 3 Output power of the CW laser versus the incident pump power

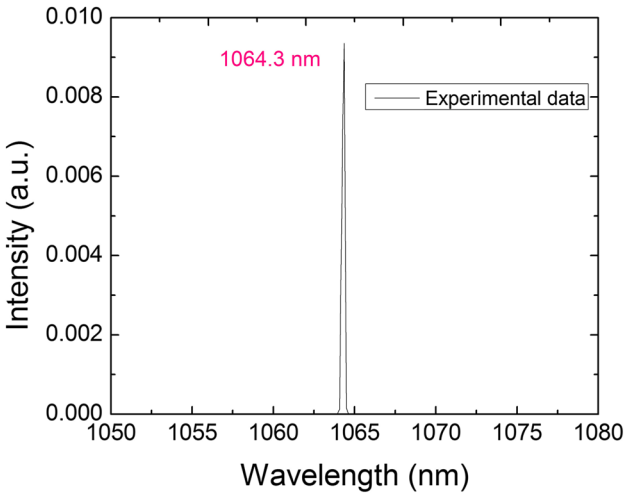

Fig. 4 Spectrum of the Q-switched laser

lower than that in the CW regime under the same pump power. This is because of the incident loss of the GNTs-SA. Compared with the previous work that used GNPs as an SA, the threshold pump power in our experiment was much lower. The good optical properties of the GNTs-SA make the threshold lower than that of other GNPs-SAs. The relationship between the incident pump power and the average output power of the Q-switched laser is shown in Fig. 5. A maximum average output power of 171 mW was achieved under a pump power of 3.48 W, corresponding to an optical-to-optical efficiency of 4.91% and a slope efficiency of 7.91%. Compared with Feng's work in Ref. [20], due to the unique structure of the GNTs, the thermal condensation of the GNTs is much weaker than that of the GNRs; thus, the maximum output power has been increased from 54 to 171 mW. As shown in Fig. 1c, compared with the SAs presented in other research, this GNTs-SA has a relatively high nonsaturable loss, which is approximately 49%. Traditionally, a high nonsaturable loss is mainly caused by crystal defects; thus, the experiment results show that it is necessary to optimize the crystal structure of the GNRs in our future work, since a high nonsaturable loss also indicates a high loss of the SA. In addition, as is known, the nonlinear saturable absorption of metal nanoparticles is contributed by the surface plasmon resonance (SPR) of the materials. However, under a high pump power, the metal particles suffer from the phenomenon of thermal condensation, which results in the deviation of the SPR absorption peak and a decrease in the absorption efficiency. In our experiment, the loss of the GNRs-SA was measured to be approximately 4.2 dB, which indicates that the low optical-to-optical conversion efficiency was mainly due to the large intracavity loss produced by the SA.

For this situation, the waveforms of the Q-switched laser were observed and were recorded at scanning times of 500 ns and 5 μs, as shown in Fig. 6. The pulse repetition rates and the pulsewidths as functions of the incident pump power are shown in Fig. 7. The pulsewidth was 1300 ns near the threshold and decreased to 275.5 ns at a pump power of 3.48 W, while the repetition rates increased with the pump power, and the maximum repetition rate was 220 kHz, corresponding to the single pulse energy of 777.3 nJ. When the pump power was larger than 3.48 W, the Q-switched laser became unstable. We did not increase the pump power to protect the GNTs-SA, and the pulsewidth was 275 ns at this moment. The gentle trend of the pulse repetition rate can be attributed to the inevitable thermal effects of the laser crystal. The pulsewidth could be further narrowed by optimizing the parameters, including shortening the cavity length and improving the modulation depth of the GNTs-SA Q-switcher.

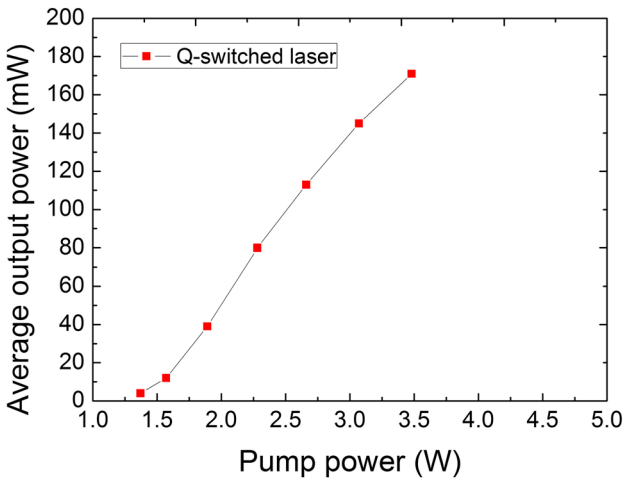

Fig. 5 Output powers versus pump power for Q-switched operation

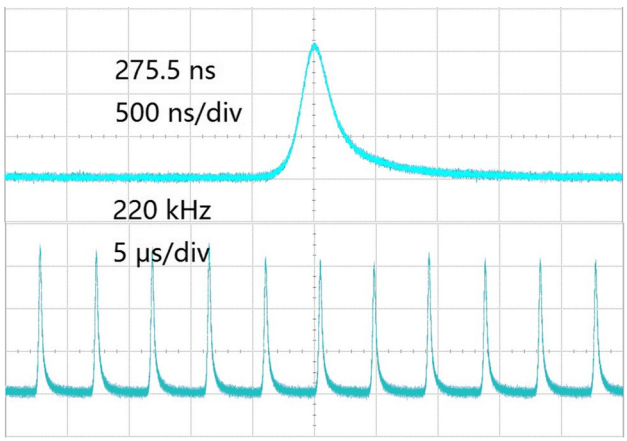

Fig. 6 Waveforms of the Q-switched lasers at scanning times of 500 ns and 5 μs

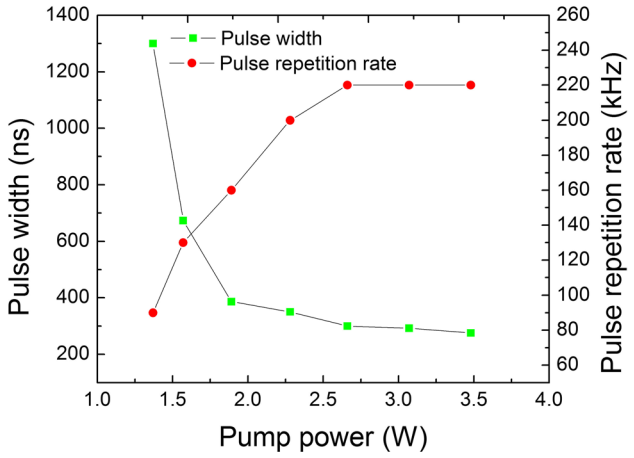

Fig. 7 Pulse repetition rates and pulsewidths versus the incident pump power

According to the experimental results, the GNTs-SA was successfully employed as a SA to achieve passively Q-switched lasers at 1.06 μm. The pulsewidth was 275.5 ns, and the threshold pump power was 1.37 W. Compared with the previous demonstration of the GNPs-based Q-switched laser, a much shorter pulsewidth and a lower threshold were achieved. If the cavity is well designed and the preparation technology of the GNTs is optimized, a better performance of the Q-switched laser will be obtained.

5 Conclusion

In conclusion, we have demonstrated for the first time a diode-pumped passively Q-switched Nd:YAG laser operating at 1064 nm with a GNTs-SA. A maximum Q-switched average output power of 171 mW was obtained under a pump power of 3.48 W, corresponding to an optical conversion efficiency of 4.91% and a slope efficiency of 7.91%. The minimum pulsewidth was 275.5 ns, and the threshold pump power was 1.38 W. To the best of our knowledge, this is the shortest pulsewidth and the lowest threshold pump power in a passively Q-switched laser at approximately 1.1 μm based on a GNPs-SA. Therefore, GNTs can be an excellent saturable absorber for Q-switched lasers.

Acknowledgements This research is supported by the National Natural Science Foundation of China (61475086) and the Foundation of Shandong Province Natural Science (ZR2015FM018 and ZR2014FM028).

Compliance with ethical standards

Conflict of interest The authors have no conflicts of interest to declare.

References

1. J.J. Degnan, IEEE J. Quantum Electron. **25**, 214 (1989)
2. H. Yu, H. Zhang, Z. Wang, J. Wang, Y. Yu, Z. Shi, X. Zhang, M. Jiang, Opt. Express **17**, 19015 (2009)
3. Y. Zhi, C. Dong, J. Zhang, Z. Jia, B. Zhang, Y. Zhang, S. Wang, J. He, X. Tao, Opt. Express **18**, 7584 (2010)
4. H. Lin, X. Meng, Y. Xu, X. Huang, H. Tan, Optik **124**, 2511 (2013)
5. Z. Yu, Y. Song, X. Dong, Y. Li, J. Tian, Y. Wang, Appl. Opt. **52**, 7127 (2013)
6. C. Li, M. Fan, J. Liu, L. Su, D. Jiang, X. Qian, J. Xu, Opt. Laser Technol. **69**, 140 (2015)
7. T. Taira, A. Kausas, L. Zheng, Lens-free microchip green laser at 1 kHz. in *Nonlinear Optics, NTu3B-2* (Optical Society of America, 2015). https://doi.org/10.1364/NLO.2015.NTu3B.2
8. M. Wang, C. Chen, C. Huang, H. Chen, Opt. Int. J. Light Electron Opt. **125**, 2154 (2014)
9. H. Chu, S. Zhao, K. Yang, Y. Li, D. Li, G. Li, J. Zhao, W. Qiao, X. Xu, J. Di, L. Zheng, J. Xu, Opt. Laser Technol. **56**, 398 (2014)
10. J.L. Xu, X.L. Li, J.L. He, X.P. Hao, Y. Yang, Y.Z. Wu, S.D. Liu, B.T. Zhang, Opt. Lett. **37**, 2652 (2012)
11. H. Long, L. Tao, C.Y. Tang, B. Zhou, Y. Zhao, L. Zeng, S.F. Yu, S.P. Lau, Y. Chai, Y.H. Tsang, Nanoscale **7**, 17771 (2015)
12. S. Wang, Y. Zhou, Y. Wang, S. Yan, Y. Li, W. Zheng, Y. Deng, Q. Zhu, J. Xu, Y. Tang, Laser Phys. Lett. **13**, 055102 (2016)
13. S. Samikannu, S. Sivaraj, Opt. Eng. **55**, 081311 (2016)
14. S. Link, C. Burda, B. Nikoobakht, M.A. El-Sayed, J. Phys. Chem. B **104**, 6152 (2000)
15. X.D. Wang, Z.C. Luo, H. Liu, N. Zhao, M. Liu, Y.F. Zhu, J.P. Xue, A.P. Luo, W.C. Xu, Opt. Commun. **346**, 21 (2015)
16. H. Zhang, J. Liu, Opt. Lett. **41**, 1150 (2016)
17. Z. Kang, X. Guo, Z. Jia, Y. Xu, L. Liu, D. Zhao, G. Qin, W. Qin, Opt. Mater. Express **3**, (2013) (1986)
18. Z. Kang, Y. Xu, L. Zhang, Z. Jia, L. Liu, D. Zhao, Y. Feng, G. Qin, W. Qin, Appl. Phys. Lett. **103**, 041105 (2013)
19. H.T. Huang, M. Li, L. Wang, X. Liu, D.Y. Shen, D.Y. Tang, IEEE Photonics J. **7**, 1 (2015)
20. C. Feng, M. Liu, Y. Li, X. Gao, Z. Kang, G. Qin, Z. Jia, X. Tao, T. Song, Y. Dun, F. Bai, P. Li, Q. Wang, J. Fang, Appl. Phys. B **123**, 81 (2017)
21. R. Boyack, E.C. Le Ru, Phys. Chem. Chem. Phys. **11**, 7398 (2009)
22. B. Nikoobakht, J. Wang, M.A. El-Sayed, Chem. Phys. Lett. **366**, 17 (2002)
23. S.B. Chaney, S. Shanmukh, R.A. Dluhy, Y.P. Zhao, Appl. Phys. Lett. **87**, 031908 (2005)
24. S. Nie, S.R. Emory, Science **275**, 1102 (1997)
25. E. Hao, G.C. Schatz, J. Chem. Phys. **120**, 357 (2004)
26. P. Pallavicini, G. Chirico, M. Collini, G. Dacarro, A. Dona, L. D'Alfonso, A. Falqui, Y. Diaz-Fernandez, S. Freddi, B. Garofalo, A. Genovese, L. Sironi, A. Taglietti, Chem. Commun. **47**, 1315 (2011)